Crystallization of Long-Chain *n*-Paraffins from Solutions and Melts As Observed by Differential Scanning Calorimetry

Xuhong Guo, Brian A. Pethica, John S. Huang, and Robert K. Prud'homme*

Department of Chemical Engineering, Princeton University, Princeton, New Jersey 08544

Received December 5, 2003; Revised Manuscript Received March 6, 2004

ABSTRACT: The crystallization of long-chain *n*-paraffins C28, C32, and C36 and of their binary mixtures from the melt and from solution in decane was investigated by differential scanning calorimetry (DSC). Both rotator and monoclinic phases were observed in crystallization from the melt, but a single monoclinic phase is observed from decane solution. The binary solution of C36 + C32 in decane forms a solid solution which shows only one thermal peak during cooling and heating, whereas C36 + C28 crystallizes separately, showing two peaks from decane solution. A solid rotator phase forms first from a mixture of C36 + C28 cooled from the melt, followed at lower temperatures by a eutectic showing separation of the paraffins in a solid-state conversion to the monoclinic forms. The addition of microcrystalline poly(ethylene−butene) (PEB) random copolymers to long-chain paraffin solutions in decane induces heterogeneous nucleation on cooling.

Introduction

Wax deposition in pipelines during production and transportation of crude oil is a major problem for the petroleum industry.[1] Most studies of wax gelation have involved visual observations,[2,3] pour-point depression measurements,[4,5] or gravimetric measurements of wax deposition.[5] Microscopy and X-ray diffraction[2,3] are powerful methods to determine the crystal structures but give limited insight into the crystallization process. Differential scanning calormetry (DSC) during crystallization monitors the phase transitions during cooling and heating and gives related thermodynamic quantities such as heat capacity and enthalpies of transition.[6] DSC has been used to investigate wax crystallization from crude oils[7−11] and from diesel fuels.[12−14] Empirical relationships were found between the wax appearance temperature (from DSC thermograms) and pour point (temperature at which the sample solidifies on cooling) or cloud point,[10,11] but the multiplicity of components and the variety of crude oils makes finding universal rules for wax formation and deposition difficult. Most DSC investigations in this field have concentrated on the crystallization of long-chain *n*-paraffins from the pure melt.[15−21] There are relatively few studies of the crystallization of long-chain *n*-paraffins from solution,[18] which is the situation of interest in crude oils. DSC observations of the effect of wax crystallization modifiers are similarly rather scarce.[22]

For the pure *n*-paraffins, two phases have been observed in the solid state: the monoclinic crystal phase at lower temperature and the disordered "rotator" or plastic phase.[23] Mueller first observed that molecules in the hexagonal phase in orthorhombic paraffin crystals rotate as rigid rods around their long axes on approaching melting temperature and hence proposed the name "rotator" phase.[24] The rotator phase has received continuous interests of both experiment and theory ever since.[21,23−27] The recent coupled FTIR/DSC study by Yoshida,[27] in particular, gives a clear demonstration of the changes in motions in the long paraffin chains on passing from the monoclinic to the "rotator" phase, which Yoshida designates as the H (hexagonal) phase.

In this paper, we examine by DSC the crystallization of single and mixed long-chain *n*-paraffins from the melt and from solution in decane and the influence of poly(ethylene−butene) (PEB) wax modifiers on crystallization from decane. We have shown that these polymers dramatically alter the gelation, rheology, and crystal morphology of wax precipitates.[33] Our neutron scattering studies have also shown that the mechanism of modification comes from cocrystallization of ethylene-rich sequences of the PEB chain into the wax.[27] The DSC method provides new insights into the role of the PEB chains on the crystal structure and modification of transitions in structure. Overall, the formation of single and binary solid paraffin phases from solution comprises a simple model system to advance the understanding and control of wax appearance from the more complex and varied crudes found in oil-field practice.

Experimental Section

Chemicals and Sample Preparation. Long-chain (LC) *n*-paraffins: octacosane (called C28 for brevity, 99%, FW 394.77, mp 59 °C), dotriacontane (C32, 97%, FW 450.88, mp 69 °C), and hexatriacontane (C36, 98%, FW 506.99, mp 74−76 °C) were purchased from Aldrich. Solutions of these long-chain *n*-paraffins or their binary mixtures were prepared in decane, also from Aldrich (anhydrous, 99+%, mp −30 °C). These chemicals were used as delivered.

Poly(ethylene−butene) (PEB) random copolymers were prepared as described previously.[28] The resulting polymers have molecular weights of ca. 7000 g/mol and a polydispersity of 1.03. Two PEBs were used in our experiments, PEB7.5 and PEB10, where the number denotes the ethyl side branches per 100 backbone carbons as determined by ^{1}H NMR.

Long-chain paraffin crystal samples were prepared from decane solution as follows: the solutions were heated to 70 °C to dissolve all the long-chain paraffins and then cooled to 0 °C at 1 °C/min. The precipitated crystals were separated by filtration with suction and dried in a vacuum at room temperature. The crystal samples were stored at ca. −4 °C before use.

Differential Scanning Calorimetry (DSC). The calorimeter used in this study is a Perkin-Elmer (Norwalk, CT) Pyris

* To whom correspondence should be addressed. E-mail: prudhomm@princeton.edu.

10.1021/ma035848x CCC: $27.50
Published on Web 06/18/2004

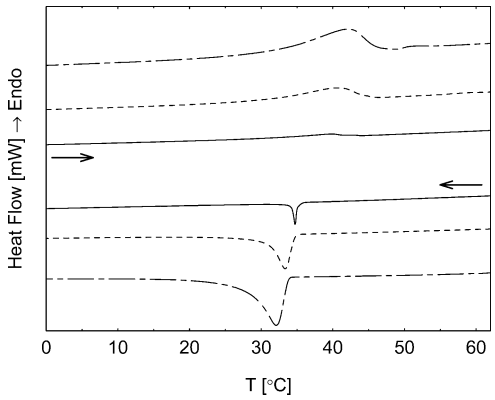

Figure 1. DSC traces of 4% C36 in decane solution at various scan rates. Upper three traces from top to bottom are for heating at 10, 5, and 1 °C/min. Lower three traces are for cooling at 1, 5, and 10 °C/min, respectively.

DSC 7 thermal analyzer system. The instrument calibrations were checked by the melting of ice from DI water and the fusion of an indium standard. The baseline was established by running an empty stainless steel pan before the sample measurement. About 10 mg of solid paraffin or its decane solution was sealed hermetically in the pan and placed on the DSC sample tray. The scanning rates (both cooling and heating) were from 1 to 10 ° C/min, and the temperature ranges were chosen to ensure that all peaks appear and that the baseline is stable for at least 10°C before the first peak and after the last peak. The sample chamber was continuously purged with dry nitrogen. The enthalpies of crystallization and melting or solution of paraffins were calculated from the area of the peaks using the Pyris software.

Results and Discussion

Single Paraffin Solutions. We began the DSC studies with solutions of C36, C32, or C28 at a weight concentration of 4% in decane. The DSC thermograms during cooling and heating of 4% C36 at several scan rates are shown in Figure 1. Only one peak appeared in all cases. X-ray diffraction at laboratory temperature showed that crystals formed from solution are monoclinic,[34] and DSC showed the rotator transition on heating these crystals in the absence of solvent, as for solid paraffins as shown below. Our DSC results show no evidence of a rotator phase or other solid structure in the formation of solid from solution or in dissolution, but we note that the relatively fast cooling and heating rates necessary with our apparatus for determining the enthalpies of crystallization may obscure more subtle crystallographic events.

The absence of a rotator phase is not surprising since the appearance temperature of solid from solution is much below the temperature range of stability of the rotator phase in the solid state in the absence of solvents.[24] The onset temperatures during cooling and peak temperatures during heating as well as the corresponded molar enthalpies are listed in Table 1. The molar enthalpies (ΔH) in all the tables are for the process of crystallization from solution or melt or for solid−solid transitions from the higher temperature to the lower temperature state. The enthalpy changes for all these transitions, as defined, are exothermic.

The crystallization peak moves to lower temperature with increased cooling rate as expected (Table 1). Further discussion will be found in the next section on the solubility of long-chain *n*-paraffins in decane. The tail of the crystallization peak at temperatures below the exothermic solidification peak becomes smoother and broader at faster cooling rates, reflecting both the thermal lag in the cooling process and the slower rate of crystal formation at lower supersaturations. The heating peak is more diffuse than the crystallization peak (which shows a sharp onset), making a solution onset temperature difficult to identify. The temperatures at peak maximum are given for the heating runs in all the tables. The peak temperatures also reflect the expected movement to higher temperature with faster heating. The estimated enthalpies of crystallization and dissolution are close except for the slowest scan rate, with its corresponding lack of sensitivity. It follows that the total amount of crystals precipitating or dissolving is independent of cooling rate and represents nearly all the initially dissolved paraffin, as will be confirmed by the temperature effect on the solubility.

Table 1. Thermal Data for 4% C36 Crystallization from Decane at Various Scan Rates

scan rate, °C/min	cooling		heating	
	T,[a] °C	$-\Delta H$, kJ/mol	T,[b] °C	$-\Delta H$, kJ/mol
1	35.1	100	39.6	95
5	34.7	103	40.5	102
10	33.7	104	42.0	101

[a] T = temperature of onset of crystallization. [b] T = peak temperature.

Table 2. Crystallization Temperatures and Enthalpies for 4% C32 and 4% C28 from Decane Solution

scan rate, °C/min	4% C32		4% C28	
	T, °C	$-\Delta H$, kJ/mol	T, °C	$-\Delta H$, kJ/mol
1	28.6	89	20.3	70
5	27.0	98	18.9	74
10	26.6	99	15.3	82

Similar phenomena were observed in the cases of 4% C32 and 4% C28 in decane, for which crystallization temperatures and ΔH data determined during cooling are given in Table 2. Comparing with the data in Table 1, the crystallization temperatures and the magnitude of ΔH shows the order of C36 > C32 > C28.

Solubility of C36, C32, and C28 in Decane. Figure 2 shows the solubilities of C36 in decane as a function of temperature as determined by different methods. The DSC appearance temperatures were measured as a function of concentration in decane at three cooling scan rates of 10, 5, and 1 °C/min. The "solubility" boundary moves toward lower temperature with increasing cooling rate as described above. A visual determination of

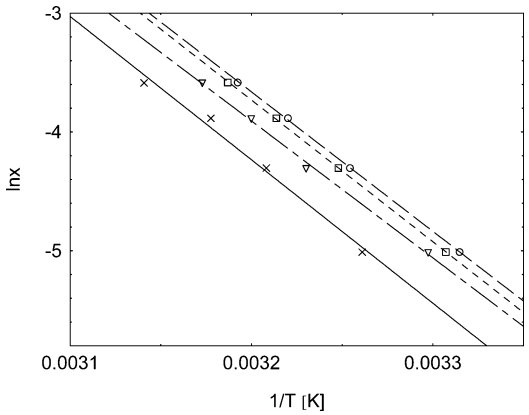

Figure 2. Solubility of C36 in decane determined by different methods. The symbols denote (○) by DSC with scan rate 10 °C/min, (□) by DSC with scan rate 5 °C/min, (▽) by DSC with scan rate 1 °C/min, and (×) visually observed.

Table 3. Standard Enthalpies and Entropies for Crystallization of C36, C32, and C28 from Decane

	C36		C32		C28	
scan rate, °C/min	$-\Delta H°$, kJ/mol	$-\Delta S°$, kJ/(mol K)	$-\Delta H°$, kJ/mol	$-\Delta S°$, kJ/(mol K)	$-\Delta H°$, kJ/mol	$-\Delta S°$, kJ/(mol K)
1	99	0.28	87	0.25	86	0.26
5	98	0.28	97	0.29	77	0.23
10	96	0.28	96	0.29	80	0.24

the crystallization temperature was performed by observing the samples 30 min after cooling in 1 °C steps,[29] an overall cooling rate somewhat less than 0.033 °C/min. The visually determined boundary is always located at a higher temperature than that from DSC with a scan rate of 1 °C/min. The apparent phase boundary, as measured by the various methods, follows the trend that the faster the rate of cooling the lower will be the measured phase boundary temperature for a given concentration.

The equilibrium solubility of long-chain *n*-paraffins can be described by the Van't Hoff equation for ideal solutions:[29,30]

$$\ln x = \frac{\Delta S^0}{R} - \frac{\Delta H^0}{R}\frac{1}{T} \qquad (1)$$

where x is the solubility, R is the ideal gas constant, T is the absolute temperature, and $-\Delta S^0$ and $-\Delta H^0$ are the standard entropy and enthalpy of crystallization, respectively. ΔS^0 and ΔH^0 for the dissolution of C36, C32, and C28 in decane were obtained from the $\ln x - 1/T$ plots of the solubility data (shown for C36 in Figure 2) according to eq 1 and are given in Table 3. In the tables, the enthalpies recorded are for formation of solids from solution or melt or for the formation of a lower temperature solid phase from a higher temperature solid phase, in all cases exothermic. The corresponding entropies are also all negative.

The ΔH^0 values determined by fitting the solubility data from DCS scans to the van't Hoff equation (Table 3) and ΔH determined by integrating under the transition peaks (Tables 1 and 2) agree to within ~3%, except for the C28 sample at the slowest scan rate. The visual method for observing crystallization onset uses stepwise cooling at an overall rate of ~0.033 °C/min. The corresponding van't Hoff plot gives $\Delta H°$ values of −101 and −93 kJ/mol for C36 and C32, again in good agreement with the results from the DSC thermal scan peaks. The earlier reported value from the "visual" method of estimating the solubilities for C28 is in poor agreement with the calorimetric values.[29]

Crystallization in the Presence of PEB. We have recently reported a new class of wax crystal modifiers based on poly(ethylene−butene) (PEB) that are effective at reducing the yield stress of the gel formed on cooling decane solutions of LC paraffins.[28] The influence of PEB on the thermal behavior of a model waxy oil is shown by comparison of DSC traces for 4% C36, 4% C32, and 4% C28 with and without PEB in decane in Figure 3.

Neither PEB10 nor PEB7.5 alone in solution shows DSC peaks during cooling and heating between −10 and 70 °C. The peaks observed in the paraffin solutions reflect the crystallization and dissolution behavior of the long-chain paraffins only. Two phenomena can be observed: the crystallization peak becomes broader and the onset smoother in the presence of both PEB10 and PEB7.5. On increasing the amount of PEBs, these phenomena become more significant (see Figure 4). It seems that the PEBs modify nucleation and growth. Small-angle neutron scattering (SANS) has shown that PEB10 and PEB7.5 self-assemble into needlelike structures or cocrystallize with long-chain *n*-paraffins to form thin sheets from decane solution.[28,31] These PEB structures appear to induce heterogeneous nucleation of long-chain *n*-paraffin crystallization in decane.

The crystallization temperatures T_c and enthalpy ΔH data determined by DSC are given in Table 4. ΔH and T_c are unchanged within experimental error by addition of PEBs. This indicates that the polymers do not alter the amount of wax that crystallizes. The effect of PEBs in modifying the gel properties which develop when the

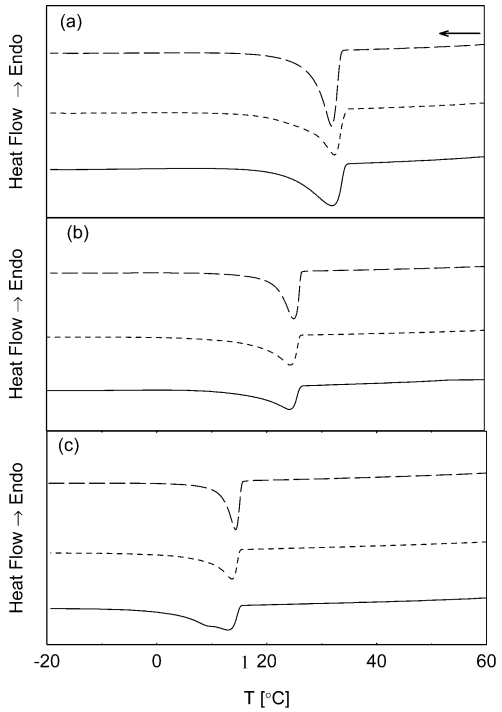

Figure 3. Comparison of DSC thermograms for 4% C36 (a), 4% C32 (b), and 4% C28 (c) in decane with 0.1% PEB10, 0.1% PEB7.5, and without PEB. Scan rate was 10 °C/min. The traces from top to bottom in each figure denote without PEB, with 0.1% PEB10, and with 0.1% PEB7.5, respectively.

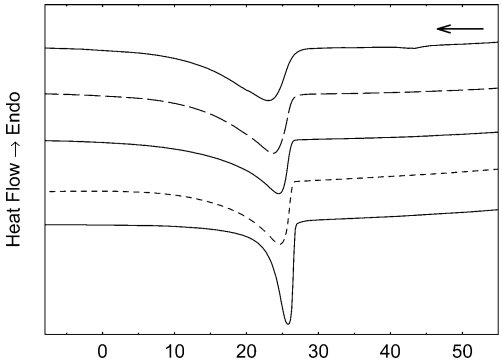

Figure 4. Effect of PEB7.5 amount on the DSC traces of 4% C32 in decane. Cooling scan rate: 10 °C/min and the curves for top to bottom denote with 0.8% PEB7.5, with 0.3% PEB7.5, with 0.1% PEB7.5, with 0.05% PEB7.5, and without PEB7.5.

Table 4. Crystallization Temperatures and Enthalpies for 4% C36, 4% C32, and 4% C28 from Decane in the Presence of 0.1% PEBs (Cooling Scan Rate: 10 °C/min)

	without PEB		0.1% PEB10		0.1% PEB7.5	
sample	T, °C	$-\Delta H°$, kJ/mol	T, °C	$-\Delta H°$, kJ/mol	T, °C	$-\Delta H°$, kJ/mol
4% C36	33.7	104	34.4	102	34.5	106
4% C32	26.6	99	26.3	92	26.3	100
4% C28	15.3	82	15.1	76	15.1	87

Table 5. Thermal Data for C36 + C32 Crystallization from Decane (Scan Rate: 10 °C/min)

	cooling		heating	
sample	T, °C	$-\Delta H$,[a] kJ/mol	T, °C	$-\Delta H$, kJ/mol
4% C36	33.7	104	42.0	101
3% C36 + 1% C32	32.3	110	38.6	102
2% C36 + 2% C32	30.5	108	36.1	100
1% C36 + 3% C32	28.4	104	34.4	101
4% C32	26.8	99	34.1	98

[a] Molecular weight of the mixture was calculated as $M = x_1M_1 + x_2M_2$, where x_i and M_i are the molar fraction and molecular weight of component i.

solid paraffins separate from decane solution relates to intercrystallite interactions, not the formation of distinctly different crystal forms.[28,29]

Mixed Paraffins in Solution. Figure 5 shows that the mixture of C36 and C32 in decane gives only one peak during both cooling and heating, indicating that C36 and C32 form a solid solution with appearance temperatures and enthalpies, as shown in Table 5. In contrast, the mixture of C36 + C28 in solution showed two peaks in the DSC traces (Figure 6), which implies that they crystallize separately.

In fact, if the components of a mixture have the same crystalline structure and the same space group, they tend to show miscibility in the solid sate.[23] But miscibility also depends on the chain length (carbon numbers n_c) of the paraffins as well as the difference of n_c between the paraffins Δn_c. According to Kravchenko's predictions,[23,32] when $\Delta n_c = 4$, two paraffins in the range of $27 < n_c < 68$ will have at least partial miscibility in the solid state. The paraffin pair C36 and C32 satisfies this requirement. The crystallization temperature and peak temperature during heating for the mixture C36 + C32 shift monotonically between those of pure C36 and C32 on changing the ratio of C36 and C32 (see Figure 5 and Table 5). The values of ΔH for the crystallization of the mixture are within experimental error intermediate between those for the single compounds.

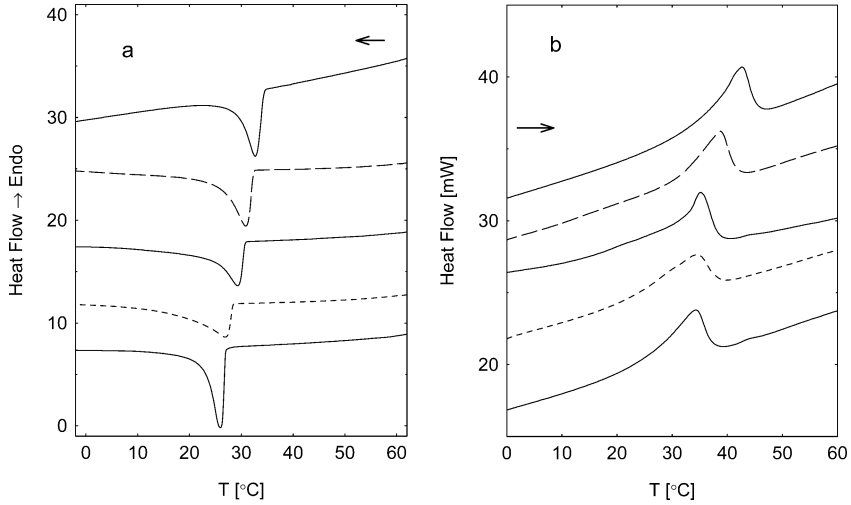

Figure 5. DSC traces of C36 + C32 mixtures in decane: (a) cooling; (b) heating. All the scan rates are 10 °C/min, and curves from top to bottom in each figure denote 4% C36, 3% C36 + 1% C32, 2% C36 + 2% C32, 1% C36 + 3% C32, and 4% C32.

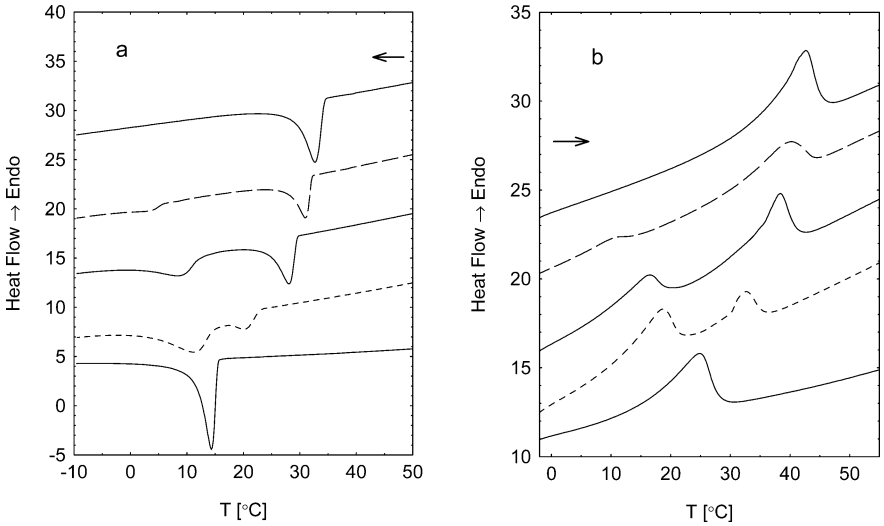

Figure 6. DSC traces of C36 + C28 mixtures in decane: (a) cooling; (b) heating. All the scan rates are 10 °C/min, and curves from top to bottom in each figure denote 4% C36, 3% C36 + 1% C28, 2% C36 + 2% C28, 1% C36 + 3% C28, and 4% C28.

Table 6. Thermal Data for C36 + C28 Crystallization from Decane (Scan rate: 10 °C/min)

	cooling				heating			
	peak I		peak II		peak I		peak II	
sample	T_1 (°C)	$-\Delta H_1$ (kJ/mol)	T_2 (°C)	$-\Delta H_2$ (kJ/mol)	T_1 (°C)	$-\Delta H_1$ (kJ/mol)	T_2 (°C)	$-\Delta H_2$ (kJ/mol)
4% C36			33.7	104			42.0	101
3% C36 + 1% C28	5.7	10[a]	32.1	86	10.1	9[a]	39.2	78
2% C36 + 2% C28	12.3	24	29.5	51	16.1	23	38.4	53
1% C36 + 3% C28	14.7	37	22.3	5[a]	18.4	33	32.5	16[a]
4% C28	15.3	82			24.6	87		

[a] Some C28 remains in solution at these temperatures.

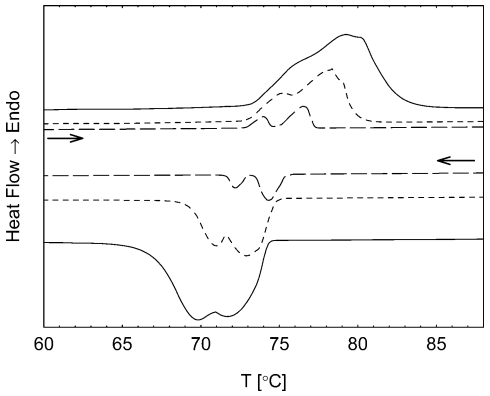

Figure 7. DSC traces for C36 at various scan rates. Symbols: (——) 10 °C/min, (- - -) 5 °C/min, and (— —) 1 °C/min.

In accordance with Kravchenko's prediction, Figure 6 indicates that little miscibility exists when $\Delta n_c = 8$ in the case of mixed C36 and C28 in decane since two peaks appear during cooling or heating. The crystallization onset temperature for each paraffin decreases as the ratio of the second paraffin in the decane solution increases at a constant 4% total wax concentration (Table 6). This tracks the solubility−temperature relation for each paraffin, as shown for C36 in Figure 2 and for C32 and C28.[29] This fact makes estimates for the molar enthalpies from the thermal peaks uncertain.

Single and Mixed Long-Chain Paraffins without Solvent. Melting and crystallization of the as-supplied paraffins C36, C32, and C28 and their binary mixtures C36 + C32 and C36 + C28 were investigated by DSC. Figure 7 shows that C36 alone shows two peaks which separate clearly when the scan rate is reduced. Upon heating, two transitions are again seen at somewhat higher temperatures, as expected. The higher temperature peaks are for the melting or formation of the rotator phase, while the lower temperature peaks are associated with the solid−solid phase transition between the monoclinic and rotator phase.[16,17,21,23,24,33,34]

The rotator phase in the absence of the solvent is also observed in the case of C32 and C28 (Figure 8). But the DSC thermograms of paraffin mixtures without decane (Figure 8) become more complicated compared with the case of the decane solutions (Figure 6). Since C36 and C32 forms solid solutions, the two separate peaks do not denote each component. The higher temperature peak is the melting of rotator cocrystals while the low-temperature peak denotes the solid−solid transition (Figure 8a).[23]

The onset temperatures and the enthalpies of the two transitions for C36 + C32 are listed in Table 7. The melting peaks associated with the monoclinic structure shift monotonically between the melting temperatures of the two components, while the solid−solid transition peak moves to lower temperature on increasing the ratio of C32 in the mixture and is located even lower than the monoclinic to rotator phase transition temperature for pure C32 in the cases of 50% C36 + 50% C32 and 25% C36 + 75% C32. These observations indicate that these two paraffins form a solid solution in the rotator phase but separate into two monoclinic phases, showing

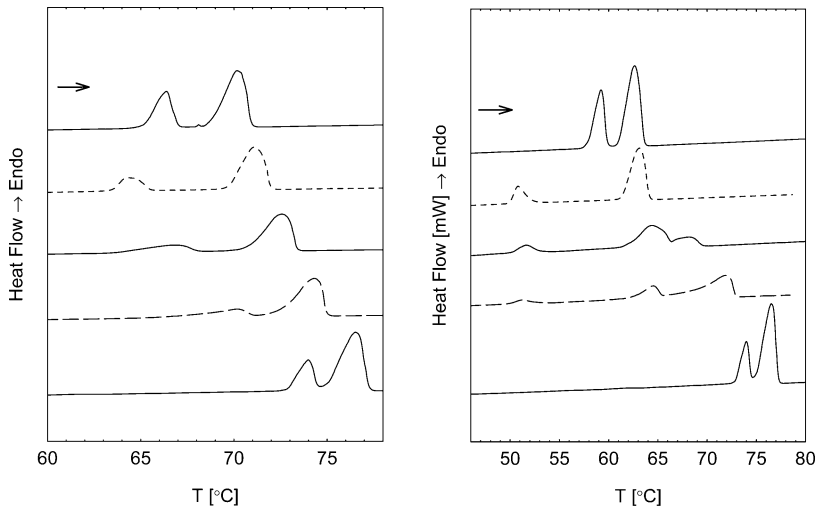

(a) C36 + C32 **(b) C36 + C28**

Figure 8. DSC traces for mixtures of C36 + C32 and C36 + C28 waxes. Crystals were formed by cooling at 10 °C/min, and the heating rate was 1 °C/min. (a) C36 + C32, curves from top to bottom denote C32, 75% C32 + 25% C36, 50% C32 + 50% C36, 25% C32 + 75% C36, and C36, respectively. (b) C36 + C28, curves from top to bottom are C28, 75% C28 + 25% C36, 50% C28 + 50% C36, 25% C28 + 75% C36, and C36, respectively.

Table 7. Thermal Data for C36 + C32 Mixtures (Heating Scan Rate: 1 °C/min)

	peak I		peak II		
sample	T_1 (°C)	$-\Delta H_1{}^a$ (kJ/mol)	T_2 (°C)	$-\Delta H_2{}^a$ (kJ/mol)	sum $-\Delta H^a$ (kJ/mol)
C36	74.9	98	72.5	39	137
75% C36 + 25% C32	72.4	78	66.9	30	108
50% C36 + 50% C32	70.2	78	63.6	23	101
25% C36 + 75% C32	69.7	75	63.5	23	98
C32	68.7	76	65.2	40	116

[a] Molecular weight of the mixture was calculated as $M = x_1M_1 + x_2M_2$, where x_i and M_i are the mole fraction and molecular weight of component *i*.

a eutectic, for the formation of the monoclinic phases. Another phenomenon is that the solid−solid transition peak for the mixture becomes broader, and $-\Delta H$ for this transition is smaller compared with that of C36 and C32, showing that the monoclinic-to-rotator transition becomes diffuse, as expected for a eutectic system, with a lower enthalpy in the mixture. Moreover, the individual components have a higher total ΔH value for the sum of the two transitions than almost all mixtures. This may be caused by the appearance of defects particularly in the monoclinic crystals due to the different chain lengths.

However, for the mixture C36 + C28, three DSC peaks appear when the amount of C36 is ≥50 wt % of the mixture (Figure 8b). C36 and C28 tend to crystallize separately from decane as discussed above, but the situation from the melt is more complex due to the presence of the rotator phase. The results of Figure 8b suggest that the C36 and C28 rotator phases, which appear first on cooling a melt, are partially miscible and that the transition to two separate monoclinic phases again shows a eutectic corresponding to peaks at lower temperatures. Dorset found that the binary mixture of C30 and C36 with $\Delta n_c = 6$ can form a solid solution, whereas C30 and C40 ($\Delta n_c = 10$) show a stable eutectic.[35] Hammami and Mehrotra reported that the C44 + C50 ($\Delta n_c = 6$) mixtures could display eutectic or isomorphous behavior depending on the thermal history during sample preparation.[36] It seems the eutectic mixture may appear in the range of $\Delta n_c = 6-10$. Therefore, it is reasonable to identify the appearance of a eutectic for the solid−solid transition from rotator to monoclinic between C36 and C28 with $\Delta n_c = 8$.

The enthalpy data for the mixtures of C36 + C28 in Table 8 are similarly complex, bearing in mind that heats of mixing in the melts and solid solutions are involved and that the integration for the enthalpies is not precise for overlapping peaks.

Long-Chain Paraffin Crystals from Decane Solutions. The heats of crystallization of the paraffins from decane solution are not affected by addition of PEBs to the solutions (Table 4). For further investigation of the potential effects of the PEBs associated with these crystals of paraffin, particularly at the rotator and melting transitions, we separated the crystals formed on cooling from the residual solvent and observed their thermal properties.

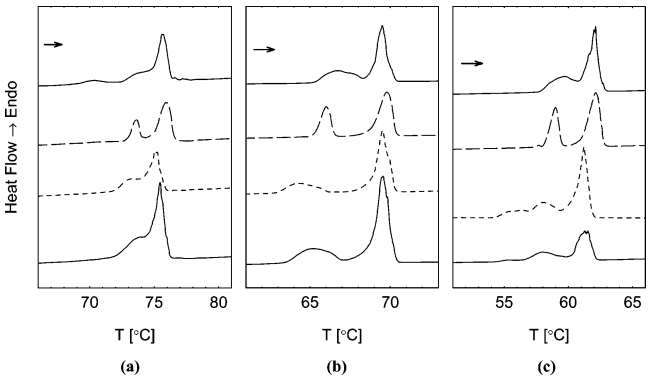

Figure 9. DSC traces for crystals samples from 4% C36, 4% C32, and 4% C28 solutions in decane. All heating scan rates are 1 °C/min. (a) C36: curves from top to bottom denote the crystals from 4% C36 (the first heating), 4% C36 (the second heating), 4% C36 + 0.1% PEB10 (the first heating), and 4% C36 + 0.1% PEB7.5 (the first heating). (b) C32: curves from top to bottom denote the crystals from 4% C32 (the first heating), 4% C32 (the second heating), 4% C32 + 0.1% PEB10 (the first heating) and 4% C36 + 0.1% PEB7.5 (the first heating). (c) C28: curves from top to bottom denote the crystals from 4% C28 (the first heating), 4% C28 (the second heating), 4% C28 + 0.1% PEB10 (the first heating), and 4% C28 + 0.1% PEB7.5 (the first heating).

Figure 9 displays the DSC heating traces for C36, C32, and C28 crystals in the absence of solvent, with or without having had wax modifier PEB10 and PEB7.5 added to their decane solutions before separation. Note that the first heating scan for DSC is for crystals directly separated from decane solution, while the second heating shows the behavior of solid paraffin formed by recooling the melt produced in the first heating in the sealed pans.

For crystals from solutions without PEBs, the first scan shows clear evidence of the solid−solid transition temperatures below the melting transition (all at temperatures well above the corresponding crystallization temperatures from decane solution), but both are less sharp than for the second heating, suggesting that the crystals direct from solution are less ordered than after melting and cooling. The first heating for C36 shows a minor peak at a temperature below the presumed rotator peak, which is absent in the second heating, again suggesting some disorder undergoing annealing. The sum of the heats in these transitions in both first or second heating is in all cases close to the heats observed with the as-received solids. The first heating of crystals formed from solutions containing PEBs again shows diffuse peaks, with the solid−solid transition at

Table 8. Thermal Data for C36 + C28 Mixtures (Heating Scan Rate: 1 °C/min)

	peak I		peak II		peak III		
sample	T_1 (°C)	$-\Delta H_1{}^a$ (kJ/mol)	T_2 (°C)	$-\Delta H_2{}^a$ (kJ/mol)	T_3 (°C)	$-\Delta H_3{}^a$ (kJ/mol)	sum $-\Delta H^a$ (kJ/mol)
C36	74.9	98	72.5	39			137
75% C36 + 25% C28	67.9	74	62.2	22	49.8	7	103
50% C36 + 50% C28	65.0	20	61.7	47	49.9	11	78
25% C36 + 75% C28	61.4	62			50.0	18	80
C28	61.0	61	57.9	33			94

[a] Molecular weight of the mixture was calculated as $M = x_1M_1 + x_2M_2$, where x_i and M_i are the mole fraction and molecular weight of component *i*.

Table 9. Thermal Data for C36 Crystals Prepared from Decane Solution (Heating Scan Rate: 1 °C/min)

crystal sample source	peak I T_1 (°C)	peak I $-\Delta H_1$ (kJ/mol)	peak II T_2 (°C)	peak II $-\Delta H_2$ (kJ/mol)	sum $-\Delta H$ (kJ/mol)
4% C36	75.4	116	68.8	19	135
4% C36[a]	74.9	89	73.0	43	132
4% C36 + 0.1% PEB10	74.6	110			110
4% C36 + 0.1% PEB7.5	74.8	112			112

[a] Second heating.

Table 10. Thermal Data for C32 Crystals Prepared from Decane Solution (Heating Scan Rate: 1 °C/min)

crystal sample source	peak I T_1 (°C)	peak I $-\Delta H_1$ (kJ/mol)	peak II T_2 (°C)	peak II $-\Delta H_2$ (kJ/mol)	sum $-\Delta H$ (kJ/mol)
4% C32	69.4	72	65.8	45	117
4% C32[a]	68.8	75	65.3	40	115
4% C32 + 0.1% PEB10	68.9	72	62.9	24	96
4% C32 + 0.1% PEB7.5	68.9	67	63.6	22	89

[a] Second heating.

Table 11. Thermal Data for C28 Crystals Prepared from Decane Solution (Heating Scan Rate: 1 °C/min)

crystal sample source	peak I T_1 (°C)	peak I $-\Delta H_1$ (kJ/mol)	peak II T_2 (°C)	peak II $-\Delta H_2$ (kJ/mol)	sum $-\Delta H$ (kJ/mol)
4% C28	60.8	60	57.7	34	94
4% C28[a]	61.0	60	58.2	33	93
4% C28 + 0.1% PEB10	60.8	57	56.4	35	92
4% C28 + 0.1% PEB7.5	60.3	53	56.5	38	91

[a] Second heating.

a somewhat lower temperature than in the absence of PEBs. More striking is that the sum of the heats of the transitions for crystals from PEB solutions is lower than in the absence of PEBs, which indicates that these polymers modify or intervene in these transitions (Tables 9−11). Elucidation of structural aspects of the polymer inclusions requires X-ray and other methods not yet applied.A first study has been made of the thermal properties of the solids formed from decane solutions containing two long-chain paraffins and PEBs. The larger number and diffuse nature of the DSC peaks for the two-component solids both complicate interpretation and increase the errors in estimating the enthalpies for individual peaks and their sums. A significant effect of PEBs was not identified.

Conclusions

The thermal behavior of long-chain *n*-paraffins and their binary mixtures during crystallization and redissolution in decane differs from the behavior observed in crystallization and melting in the absence of solvent. Heating the solids or cooling the melts of single component paraffins shows the solid−solid rotator/monoclinic transition peaks in the DSC traces, but from decane no rotator phase is seen during crystallization since the onset temperature for crystallization is well below that for the solid−solid transition seen on cooling melts. The crystals from a mixture C36 + C32 in decane form a solid solution which shows only one DSC peak on crystallization. A mixture of C36 and C32 crystallizes from the melt in the absence of solvent to give solid solutions in both the rotator and monoclinic phases. In contrast, mixtures of C36 + C28 crystallize separately by displaying two DSC peaks from solution and three from the melt. Mixtures of C36 and C28 from the melt first form a mixed rotator phase as the temperature falls and then show a eutectic for the solid−solid transition to the monoclinic form, indicating separation of the two long-chain alkanes in the monoclinic state. The DSC traces on heating decane-free crystals formed from solution in decane show some evidence of disorder compared to crystals from the melt but display the rotator phase clearly before melting. Addition of PEB polymers to solutions of the long-chain paraffins in solution shows minor effects on the DSC Pattern for crystallization or redissolution. Decane-free Crystals formed from decane solutions in the presence of PEBs show significant decreases in the sum of the enthalpies of the solid−solid and melting transitions, as compared to crystals formed in the absence of the polymers. Polymer inclusion appears to modify or disorder the crystals from decane. When these same crystals are melted and then cooled, the subsequent thermal behavior on heating to the melt is quite similar to that for the original pure paraffins. The solubility of long-chain *n*-paraffins in decane is well described by the van't Hoff equation, giving heats of solution in agreement with the calorimetric estimates.

Acknowledgment. We gratefully acknowledge support from the Halliburton Co.

References and Notes

(1) Misra, S.; Baruah, S.; Singh, K. *SPE Products & Facilities* **1995**, *10*, 50.
(2) Edwards, R. T. *Ind. Eng. Chem.* **1957**, *49*, 750.
(3) Chichakli, M.; Jessen, F. W. *Ind. Eng. Chem.* **1967**, *59*, 86.
(4) Venkatesan, R.; Singh, P.; Fogler, H. S. *SPE J.* **2002**, *7*, 349.
(5) Sifferman, T. R. *J. Pet. Technol.* **1979**, 1042.
(6) Hoehne, G.; Hemminger, W.; Flammersheim, H.-J. *Differential Scanning Calorimetry, an Introduction for Practitioners*; Springer: Berlin, 1996.
(7) Faust, H. R. *Thermochim. Acta* **1978**, *26*, 383.
(8) Stank, J.; Mullay, J. *Thermochim. Acta* **1986**, *105*, 9.
(9) Letoffe, J. M.; Claudy, P.; Kok, M. V.; Garcin, M.; Volle, J. L. *Fuel* **1995**, *74*, 810.
(10) Rademeyer, M.; Dorset, D. L. *J. Phys. Chem. B* **2001**, *105*, 5139.
(11) Jiang, Z.; Hutchinson, J. M.; Imrie, C. T. *Fuel* **2001**, *80*, 367.
(12) Gimzewski, E.; Audley, G. *Thermochim. Acta* **1993**, *214*, 149.
(13) Craig, S. R.; Hastie, G. P.; Roberts, K. J.; Sherwood, J. N.; Tack, R. D.; Cernik, R. J. *J. Mater. Chem.* **1999**, *9*, 2385.
(14) Coutinho, J. A. P.; Dauphin, C.; Daridon, J. L. *Fuel* **2000**, *79*, 607.
(15) Hammami, A.; Mehrotra, A. K. *Thermochim. Acta* **1993**, *215*, 197.
(16) Sirota, E. B.; Singer, D. M. *J. Chem. Phys.* **1994**, *101*, 10873.
(17) Hammami, A.; Mehrotra, A. K. *Fuel* **1995**, *74*, 96.
(18) Coutinho, J. A. P.; Ruffier-Meray, V. *Ind. Eng. Chem. Res.* **1997**, *36*, 4977.
(19) Gilbert, E. P. *Phys. Chem. Chem. Phys.* **1999**, *1*, 1517.
(20) Severtson, S. J.; Nowak, M. J. *Langmuir* **2001**, *17*, 4990.
(21) Nowak, M. J.; Severtson, S. J. *J. Mater. Chem.* **2001**, *36*, 4159.
(22) Kim, J. K.; Kim, B. *J. Polym. Sci., Part B: Polym. Phys.* **1999**, *37*, 1991.
(23) Dirand, M.; Bouroukba, M.; Chevallier, V.; Petitjean, D.; Behar, E.; Ruffier-Meray, V. *J. Chem. Eng. Data* **2002**, *47*, 115.
(24) Ungar, G. *J. Phys. Chem.* **1983**, *87*, 689.
(25) Sirota, E. B.; Herhold, A. B. *Science* **1999**, *283*, 529.
(26) Sirota, E. B. *Phys. Rev. E* **2001**, *64*, 507011.

(27) Yoshida, H. J. *Therm. Anal. Calorim.* **1999**, *57*, 679.
(28) Ashbaugh, H. S.; Radulescu, A.; Prud'homme, R. K.; Schwahn, D.; Richter, D.; Fetters, L. J. *Macromolecules* **2002**, *35*, 7044.
(29) Ashbaugh, H. S.; Fetters, L. J.; Adamson, D. H.; Prud'homme, R. K. *J. Rheol.* **2002**, *46*, 763.
(30) Beiny, D. H. M.; Mullin, J. W.; Lewtas, K. *J. Cryst. Growth* **1990**, *102*, 801.
(31) Schwahn, D.; Richter, D.; Lin, M.; Fetters, L. J. *Macromolecules* **2002**, *35*, 3762.
(32) Kravchenko, V. *Acta Physicochim. URSS* **1946**, *21*, 335.
(33) Doucet, J.; Denicolo, I.; Craievich, A.; Collet, A. *J. Chem. Phys.* **1981**, *75*, 5125.
(34) Guo, X.; Pethica, B. A.; Huang, J. S.; Prud'homme, R. K.; Adamson, D. H.; Fetters, L. J., submitted to *Energy Fuels*.
(35) Dorset, D. L. *Macromolecules* **1986**, *19*, 2965.
(36) Hammami, A.; Mehrotra, A. K. *Fuel* **1996**, *75*, 500.

MA035848X